

Report

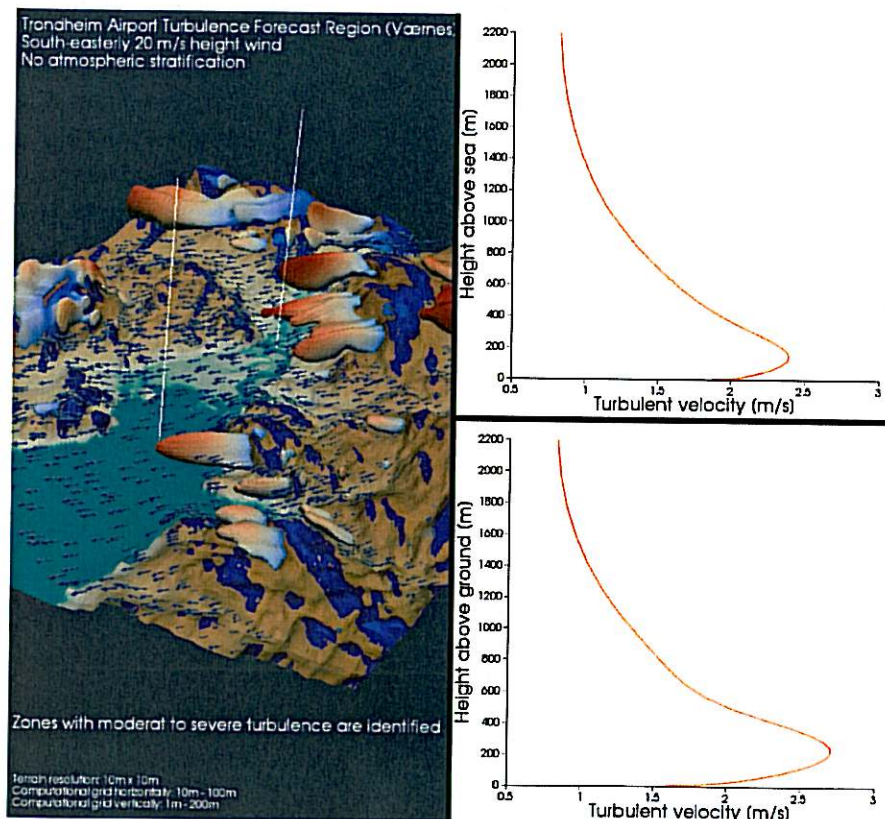
Terrain-forced Wind and Turbulence and Optimization of Local Domains and Grids for Terrain-induced Turbulence Forecast

Case studies of four Norwegian airports

Author(s)

Karstein Sørlø

Adil Rasheed



SINTEF IKT
SINTEF ICTAddress:
Postboks 4760 Sluppen
NO-7465 Trondheim
NORWAYTelephone:+47 73593000
Telefax:+47 73592971postmottak.ikt@sintef.no
www.sintef.no
Enterprise /VAT No.
NO 948 007 029 MVA

Report

Terrain-forced Wind and Turbulence and Optimization of Local Domains and Grids for Terrain-induced Turbulence Forecast

KEYWORDS:Airport
Terrain
Turbulence
Numerical forecast
Grid optimization**VERSION****DATE**

2011-07-05

AUTHOR(S)Karstein Sørli
Adil Rasheed**CLIENT(S)**

Avinor AS

CLIENT'S REF.

Erling Bergersen

PROJECT NO.

90A344

NUMBER OF PAGES/APPENDICES:

38

ABSTRACT

A study of mountain-forced wind, wind-shear and turbulence was conducted in order to reveal general characteristics of terrain-induced turbulence nearby airports in mountainous areas. Special studies of the topography close to a number of Norwegian airports that currently receive hourly forecasts of terrain-induced turbulence were also performed. It was found that there is a potential for improving efficiency and robustness as well as accuracy of the *micro-scale* code at the end of the nested set of numerical weather prediction codes that each resolves different scales, and being used in the forecasting mentioned. The optimizing was done by tuning the shape, size and orientation of the local regions as well as the quality of the spatial grid within the regions.

The continuous increase of computational power opens for utilizing finer and larger forecast grids for airport regions with topography that are not resolved with the present grids. This gives promise to using these finer micro-scale grids in operational forecasting in near future. A rough estimate of the present realistic and operational grids is a doubling of grid density horizontally as well as increasing grid density vertically by a factor 1.5 as compared with existing numbers.

The selected airports were investigated in order to deduce general as well as specific guidelines regarding optimum size, shape and orientation of the micro-scale forecast region relative to the local topography nearby the airports. Details for the selected airports are found in the conclusion section of the report.

PREPARED BY

Karstein Sørli

SIGNATURE**CHECKED BY**

Hans Erik Swendgård

SIGNATURE**APPROVED BY**

Roger Bjørgen

SIGNATURE for R. Bjørgen**REPORT NO.**

SINTEF A19928

ISBN

978-82-14-04987-9

CLASSIFICATION

Unrestricted

CLASSIFICATION THIS PAGE

Unrestricted

Contents

1	Introduction	5
2	Terrain-forced airflow	6
2.1	Topographic of the terrain	7
2.2	Eddies, wakes and vortices	11
2.3	Flow over mountains	13
2.3.1	Mountain waves, lee waves and hydraulic flows	13
2.4	Flow around mountains	17
2.5	Flows through gaps, channels and passes	17
2.5.1	Flows through coastal mountain ranges	17
2.5.2	The Venturi (or Bernoulli) effect	18
2.5.3	Forced channeling	18
2.6	Blocking, cold air damming and obstruction of air masses	18
3	Turbulence in the neighborhood of airports	20
3.1	Windshear and turbulence	20
3.2	Horizontal and vertical windshear and effects on aircrafts	21
4	Optimizing local forecast regions	23
4.1	Digital elevation models	24
4.2	Airflow simulation code	25
4.3	Results of studying four Norwegian airports	26
4.3.1	Trondheim Airport Værnes - 17 m ASL RWY 09/27	26
4.3.2	Sandnessjøen Airport Stokka - 17 m ASL RWY 03/21	27
4.3.3	Tromsø Airport Langnes - 10 m ASL RWY 01/19	28
4.3.4	Hammerfest Airport - 81 m ASL RWY 05/23	29
5	Conclusion	31

List of Figures

1	The dividing streamline height is the height of the boundary between low-level air, which splits to flow around the barrier, and upper level air, which is carried over the barrier. (Ref. [Whiteman (2000)])	7
2	Under stable conditions, winds split around an isolated mountain, and strong wind zones are produced on the edges of the mountain that are tangent to the flow. (Ref. [Whiteman (2000)])	8
3	The orientation and shape of a ridgeline affect the speed and direction of a flow crossing a mountain barrier. The highest speedups occur over ridgelines that are perpendicular to the flow or have a concavity oriented into the flow. (Ref. [Whiteman (2000)])	9
4	Flow separations occur on the windward or leeward faces of steep-sided hills or mountains. A flow separation on the windward side occurs below the dashed green line. A smaller flow separation is also present on the lee side. (Ref. [Whiteman (2000)])	10
5	Vortex pairs and a wake are generated by the flow around a mountain. (Ref. [Whiteman (2000)])	12
6	Stably stratified air that is lifted over mountains oscillates about its equilibrium level on lee side of the mountain, producing waves [Whiteman (2000)].	13
7	Vertically propagating mountain waves have highest amplitudes far above the mountains. High lenticular clouds are often indicators of these waves. These waves can generate moderate to severe turbulence [Whiteman (2000)].	14
8	Trapped lee waves reach their highest amplitudes in a confined layer on the lee side of the mountains. Regularly spaced low-altitude lenticular clouds are the best indicators of trapped lee waves. These waves can generate moderate to severe turbulence [Whiteman (2000)].	15
9	Waves can be (a) amplified or (b) canceled by successive ridges, depending on the relationship between the ridge separation distance L and the wavelength A of the flow [Whiteman (2000)].	16
10	The Venturi effect causes a jet to form as winds pass through a terrain constriction and strengthen [Whiteman (2000)].	19
11	Channeling occurs when upper winds are brought down into valleys from aloft and turned to flow along the valley's longitudinal axis [Whiteman (2000)].	19
12	Sketch showing affect of windshear during aircraft descent into an airport (NASA) (Ref. http://en.wikipedia.org/wiki/File:Windshearaircraftnasa.gif)	22
13	Horizontal windshear and it's effect on an aircraft's flight path.	23
14	Vertical windshear and it's effect on an aircraft's flight path.	24
15	Digital terrain data for the <i>Værnes</i> region. The plot is using a logarithmic scale in order to highlight lower elevations.	25

- 16 This figure shows the results of analyzing the sensitivity to regional rotation at Værnes. The upper left and lower left images show iso-surfaces of turbulent velocity indicating moderate turbulence to severe turbulence for no rotation and a counterclockwise rotation of 45° , respectively. The curves on the right side show the associated turbulent velocities for both cases along a vertical line located in the fjord right through the gliding path of aircrafts approaching the runway from the west. Note the larger extent of the turbulence area as well as the larger maximum value of the turbulent velocity in the case of regional rotation. 27
- 17 The figure shows topography around the airport at Værnes looking towards the valley *Stjørdalen*, and turbulent velocity iso-surfaces ($ut=3.0$) using four different grid resolutions. Typically, doubling the grid density horizontally makes a significant improvement to north of the hillside *Gjevingåsen* and further east into the valley of *Stjørdalen*. These areas are crossing the approach path of aircrafts both on the western and the eastern side of the airport. 28
- 18 This figures illustrates the sensitivity of predicted turbulent velocity to the size and location of the forecast region at Værnes. From left to right the regions are 12×12 , 16×16 , 20×20 and 24×24 kilometers of extension horizontally, all of which coincide in the north-east corner. 29
- 19 The figure illustrates a worst case scenario at Stokka when strong wind is forced to cross over the relatively long, high and "wavy" mountain-ridge of *De syv søstre*. The simulation is done without atmospheric stratification. With a stable atmosphere, mountain waves are easily generated with *rotors* on the lee side of the mountain, resulting in severe turbulence. 30
- 20 This figure shows terrain and predicted severe turbulence ($ut=3.5$) at Stokka for south-easterly wind crossing the mountain-ridge with speed 20 m/s aloft. Neutral atmosphere. 31
- 21 Sensitivity of turbulence velocity to grid density at Stokka. A doubling of the number of grid points horizontally (both directions) and increasing the number of grid points vertically by a factor 1.25, "moves" the severe turbulence zones closer to the airport. Also note the wavy turbulent regions over the mountain-ridge. 32
- 22 This shows a close-up of the results of Figure 21 for Stokka airport. Note the approaching front of severe turbulence resolved by the finer grid of $211 \times 211 \times 51$ points. Also note the sharper and higher peak of the turbulent velocity curve along a vertical line approximately a the middle of the runway location, for the denser grid case. 33
- 23 Initial simulation of terrain-induced turbulence at Langnes in Tromsø. Note that close to light turbulence is predicted at higher elevations than for the previous airports. The curve on the right side shows turbulent velocity along a vertical line located at the runway. 34

LIST OF FIGURES

24	This figure shows terrain and regions of light to moderate turbulence at Langnes. Further explanations in the figure.	35
25	Tromsø Airport Langnes. West-southwesterly wind 20 m/s aloft and idealized wind profile at inflow boundaries. Illustration of the channeling effect at different levels. Also note the variation of the vertical component at the various levels.	36
26	Terrain and predicted turbulent regions at Hammerfest Airport for north-westerly winds crossing the hillside on the NW side of the airport. A region of moderate turbulence is predicted at the location of the runway.	37
27	Sensitivity of turbulent zones to grid density at Hammerfest Airport. Note the different maximum values of turbulent velocity along a vertical line at the airport for the coarse and fine grid.	38

1 Introduction

Currently there are nineteen Norwegian airports with a local turbulence forecast system installed and in daily operations. The size of the local domain around the airports is approximately $30 \times 30 \text{ km}^2$ horizontally and between 3 and 5 km vertically, the size being based mainly on available computational resources at the time of the first installations that were done some years ago.

With a few exceptions, the shape of the local airport regions are quadratic and oriented W-E-S-N. The exceptions are characterized by some stretching and rotation of the default size and shape. Stretching and/or rotation is done in order to catch terrain effects and critical wind directions in a better way. For some topographies and critical wind directions it is also done to reduce numerical diffusion of conserved quantities (mass, momentum, thermal and turbulent kinetic energy) of the mathematical model. So far the vertical extension of the domains are determined by the highest mountain within the forecast region. Normally, the height of the *micro-scale*¹ forecast region is chosen to be approximately five times the highest mountain peak within the region.

These design criteria for an actual forecast region are based on experience and knowledge of physical processes in the atmosphere and have shown to work properly in most cases. However, there are indications that the criteria may be tuned so that we can obtain even better performance with respect to robustness and numerical accuracy of the micro-scale turbulence forecast modeling software. Therefore, the main objective of the present work is to perform a thorough analysis of selected airports in order to optimize both their regional extension and orientation as well as their discretization (grid). The main variables of concern are (i)critical wind direction, (ii)local terrain, and (iii)coupling with the mesoscale model. In addition to optimizing existing forecast regions, the results of the study may be used as guidelines for putting new forecast locations into operation.

The method of choice would be determining *the sensitivity of turbulence forecasts* to control parameters like *domain extension*, *domain rotation* and *grid density* by utilizing a certain type of sensitivity equations. Earlier tests (see [Utne & Sørli (2008)] and [Utne & Sørli (2009)]) of this kind of method on simplified 2D problems showed very promising results. However, it remains to implement and test this method on realistic 3D airport regions. This is planned for future work. In this report are described the results of optimizing domain and grid for selected airports, using a less stringent but proven approach. It is characterized by the analysis of the particular topography and critical wind directions by conducting selected simulations for different boundary locations, orientations, and grid resolutions. Finally the results are compared, focusing on aircraft glide paths, thresholds and landing spots on the runway of the actual airports.

Before going on with the main objectives of the present work as described above, an introduction to terrain-forced airflow is given in the next section. A study of mountain-forced wind, wind-shear and turbulence was conducted in order to reveal general characteristics of

¹*Micro-scale* atmospheric flow is the study of short-lived atmospheric phenomena with spatial scales less than 1 km. In the present work these are the scales resolved by the SIMRA code.

terrain-induced turbulence nearby airports in mountainous areas.

For previous reports on this subject it is referred to [Eidsvik & Utne (2006)] which analyzes a plane crash in Hammerfest in 2005. That specific event actually triggered the development of the present turbulence forecast system. It is also referred to the reports [Eidsvik (2006a), Eidsvik (2006b), Eidsvik (2006c)] for details on the subject of predicting local atmospheric flow. In the papers [Eidsvik & Holstad & Lie & Utne (2004)] and [Eidsvik (2008)] the early characteristics of the prediction system for terrain-induced turbulence mentioned above is described with respect to overall functionality and estimates of prediction errors, respectively. For a thorough description of the basics regarding modeling and simulation of stratified geophysical flows over complex topographies it is referred to [Utne (2007a)].

A new paper is under preparation that describes the present turbulence forecast system including mathematical models, numerical algorithms, nesting of models, operational issues, and validation.

2 Terrain-forced airflow

Terrain-forcing may cause airflow approaching a mountain barrier to be carried over, diverted around, forced through gaps, or to be completely blocked. The main factors determining the behavior of an approaching flow in response to a mountain barrier are:

- the stability of the approaching air,
- the speed of the airflow, and
- the topography of the terrain.

Unstable or neutrally stable air is easily carried over a mountain barrier. We can think of *air stability* as the tendency for air to rise or fall through the atmosphere under its own "power". Stable air has a tendency to resist movement. On the other hand, unstable air will easily rise. The behavior of stable air approaching a mountain barrier depends on the degree of stability, the speed of the approaching flow, and the terrain characteristics. The more stable the air, the more resistant it is to lifting and the greater the likelihood that it will flow around, be forced through gaps, or be blocked by the barrier. A layer of stable air can split, with air above the dividing streamline height flowing over the mountain barrier, and air below this streamline, splitting upwind of the mountains, flowing around the barrier (figure 1), and reconverging on the leeward side. A very stable approaching flow may be blocked on the windward side of the barrier. Moderate to strong cross-barrier winds are necessary to produce terrain-forced flows. Unstable and neutral flows are easily lifted over mountain barriers, even by moderate winds, but strong cross-barrier winds are needed to carry stable air over a mountain barrier. As the speed of the cross-barrier flow increases, the amount of stable air carried over the barrier also increases, with less air channeled around or through barrier gaps and less air blocked upwind of the barrier.

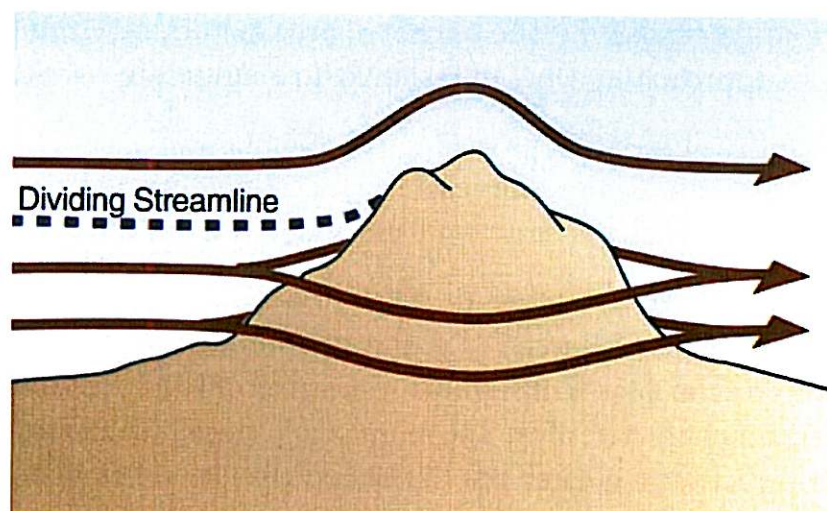


Figure 1: The dividing streamline height is the height of the boundary between low-level air, which splits to flow around the barrier, and upper level air, which is carried over the barrier. (Ref. [Whiteman (2000)])

2.1 Topographic of the terrain

A number of terrain characteristics influence both the speed and the direction of terrain-forced flows. The height and length of the mountain barrier can determine whether air goes over or around the barrier. The amount of energy required for air to flow over a high mountain ridge is much greater than that required to flow over a small hill. More energy is required to flow around an extended ridge than around an isolated peak. Thus, high windspeeds are required to carry air over a high mountain range or around an extended ridge. When stable air flows around an isolated peak or the edges of an elongated mountain range, the highest wind speeds are on the hillsides where the flow is parallel to the peak's contour lines (figure 2). In performing 3D airflow simulations it's evident that the given terrain and grid resolution will be important in order to predict a realistic flow-field close to a mountain peak. If the resolution is too coarse the peak will easily be "cut-off" and the wind speeds will be under-estimated at the actual location of the peak, even if the energy or momentum upstream is large enough to bring it the right level at this location. ²

The shape of the vertical cross section through the mountain barrier affects wind speed on both the windward and leeward sides. Windspeed increases at the crest of a mountain,

²The last comments are related to a recent analysis and validation of models against wind measurements on a mountain close to Langnes.

with gently inclined triangular-shaped hills producing the greatest increase in speed, flat-topped mountains producing the smallest increases, and rounded mountaintops producing intermediate speedups. Flow separations or separation eddies can form over steep slopes or cliffs on either the windward or leeward sides of a barrier. These elongated, horizontal-axis eddies, which can extend along the entire length of the barrier, reduce near-ground wind speeds over the slopes (figure 4). The flow above these separation eddies, however, speeds up as it crosses the barrier. The orientation of a mountain ridge relative to the

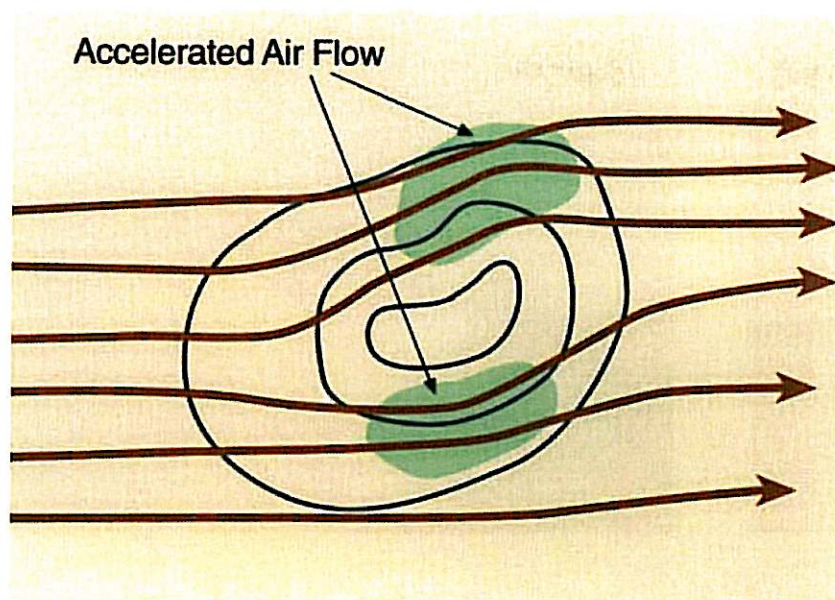


Figure 2: Under stable conditions, winds split around an isolated mountain, and strong wind zones are produced on the edges of the mountain that are tangent to the flow. (Ref. [Whiteman (2000)])

approaching flow and the curve of the ridgeline (as viewed from above) affect wind direction and speed. Ridgelines that are concave to the windward side and mountain barriers oriented perpendicular to the flow cause flow across the barrier to increase and frequently generate lee waves downwind of the obstacle. A good example is the *De syv søstre* close to Stokka airport. In this case, south-easterly airstreams approach this mountain ridge perpendicular and are forced to cross the ridge and result in lee waves. In addition, the ridgeline is quite rugged which creates disturbances in the flowfield and that easily contributes to the generation of turbulence.

Flows approaching barriers with ridgelines that are parallel to, oblique to, or convex to the approaching flow (figure 3) change direction to follow the underlying terrain and generate lee waves less frequently. Smaller scale features on a ridgeline can also affect the approaching flow, channeling winds through passes and gaps. The presence of valleys and

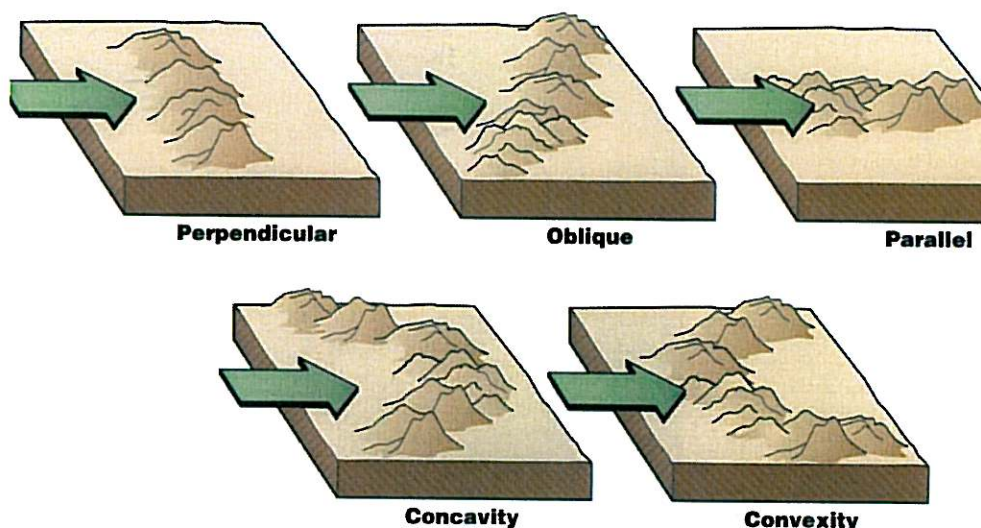


Figure 3: The orientation and shape of a ridgeline affect the speed and direction of a flow crossing a mountain barrier. The highest speedups occur over ridgelines that are perpendicular to the flow or have a concavity oriented into the flow. (Ref. [Whiteman (2000)])

fjords affects wind speed. This is a typical topographic terrain scenario for many of the Norwegian airport nearby regions. Sites low in a valley and in fjords are often protected from prevailing winds by the confining topography. If winds aloft are strong, however, eddies can form within a valley or basin downwind of a ridgeline, bringing strong, gusty winds to lower elevations.

The roughness of the underlying surface affects wind speed. The rougher the surface, the greater is the reduction in wind speed. Wind speeds increase when airstreams move from a rough surface to a smooth surface (e.g., from a rough, mountainous area onto an estuary, fjord or ocean bay) and decrease when winds move from a smooth surface to a rough surface. The layer in which wind speeds are affected by a roughness boundary becomes deeper with distance downwind from the roughness boundary. An abrupt increase in roughness causes winds to converge, and air to rise. Finally, terrain obstacles (mountains, forests, trees, buildings) generate turbulent eddies and/or wakes when the approaching flow has sufficient speed. Eddies are swirling currents of air at variance with the main current. A wake forms when eddies are shed off an obstacle and cascade into smaller and smaller scales. Wakes may also form when air splits to flow around columns of warm air or convective towers in

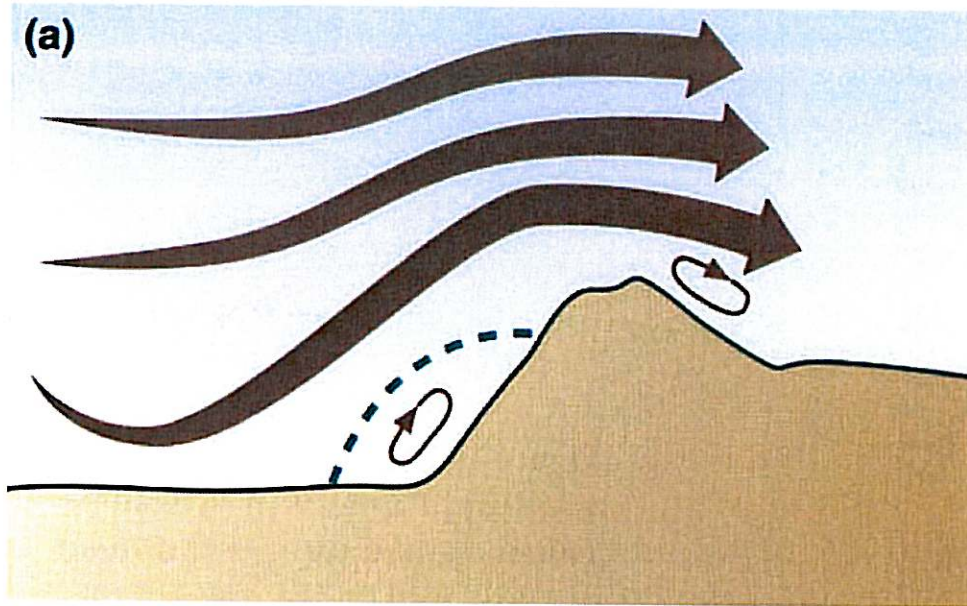


Figure 4: Flow separations occur on the windward or leeward faces of steep-sided hills or mountains. A flow separation on the windward side occurs below the dashed green line. A smaller flow separation is also present on the lee side. (Ref. [Whiteman (2000)])

thunderstorms. These wakes are characterized by low wind speeds, but their high turbulence can produce locally gusty winds.

Approaching flows that are carried over mountains respond to overall or large-scale features of the topography rather than to small-scale topographic details. In fact, when a low-lying cold air mass is present on the windward and/or leeward sides of the mountain barrier, the approaching flow responds to the combination of the actual terrain and the adjacent air mass. Thus, the effective topography that influences the approaching flow can be higher and wider than the actual topography. Terrain-forced flows respond to both topography (mountain valleys, passes, plateaus, ridges as well as fjords) and roughness elements (mountain peaks, terrain projections, trees, and other smaller terrain variations) in complex terrain. Wind speeds can vary significantly between sites exposed to prevailing winds or terrain-forced flows and sites protected from winds by the terrain.

2.2 Eddies, wakes and vortices

Eddies can form anywhere in the atmosphere, both at the ground and aloft, in relationship to obstacles and over unobstructed terrain as the result of wind shear or convection. The relative horizontal and vertical dimensions of an eddy are determined by the stability. *Isotropic* eddies³ develop in neutral stability, whereas vertically suppressed eddies develop in more stable air, and vertically enhanced eddies form in unstable air.

A wake is an area extending downwind of an obstacle and is characterized by relatively slower wind speeds but increased gustiness. Winds are generally slowed downwind of obstacles to distances roughly 20 times the obstacle height, although velocity reductions in wakes have been detected as much as 60 obstacle-heights downwind.

Vortices, whirling masses of air in the form of a column or spiral, usually rotate around either vertical or horizontal axes. Vertical-axis vortices in the atmosphere range in size from *dust devils*, which is a strong and relatively long-lived whirlwind, ranging from about half a meter wide and a few meters tall to more than 10 meters wide and more than 1000 meters tall, to tornadoes, hurricanes and synoptic-scale high and low pressure centers. Horizontal-axis vortices are caused by vertical wind shear and turbulence and are common in the lee of extended terrain obstacles such as mountain ridges. Horizontal-axis vortices can be stretched into vertical-axis vortices by convection when the ground is heated and the atmosphere is unstable.

For further details regarding mountain meteorology we have included some selected topics from [Whiteman (2000)] in the following sections.

³Eddies that have similar vertical and horizontal dimensions

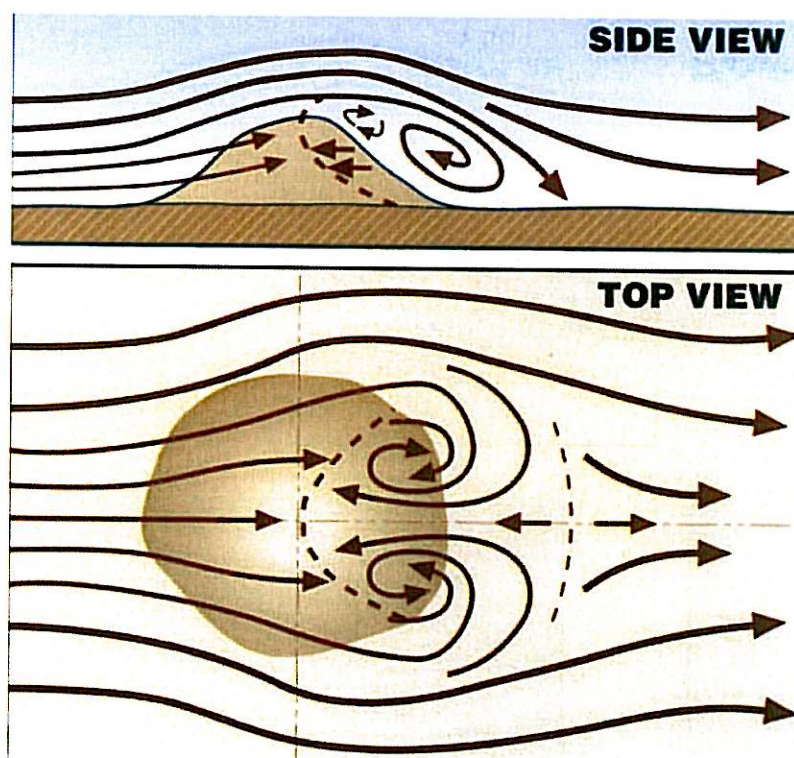


Figure 5: Vortex pairs and a wake are generated by the flow around a mountain. (Ref. [Whiteman (2000)])

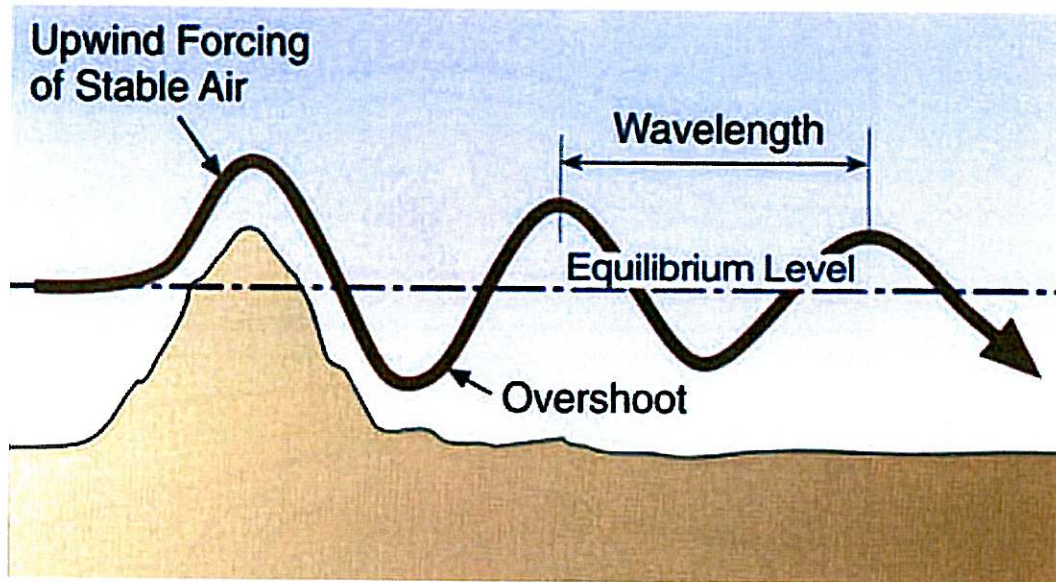


Figure 6: Stably stratified air that is lifted over mountains oscillates about its equilibrium level on lee side of the mountain, producing waves [Whiteman (2000)].

2.3 Flow over mountains

An approaching flow tends to go over a mountain barrier rather than around it if the barrier is long, if the cross-barrier wind component is strong, and if the flow is unstable, near-neutral, or only weakly stable. Flow over mountains generates mountain waves and lee waves in the atmosphere and can produce downslope windstorms.

2.3.1 Mountain waves, lee waves and hydraulic flows

As stable air flows over a mountain range, gravity waves (i.e., vertical waves in the atmosphere created as gravity acts on local variations in air density) can be generated either over the mountains or in the lee of the mountains. Stable air that is lifted over a mountain barrier cools, becomes denser than the air around it, and, under the influence of gravity, sinks again on the lee side of the barrier to its equilibrium level. The air overshoots and oscillates about its equilibrium height (see Figure 6). Gravity waves that form over the mountains are called *mountain waves*. Mountain waves have a tendency to propagate vertically and can thus be found not only at low levels over hills and mountains but throughout the troposphere and

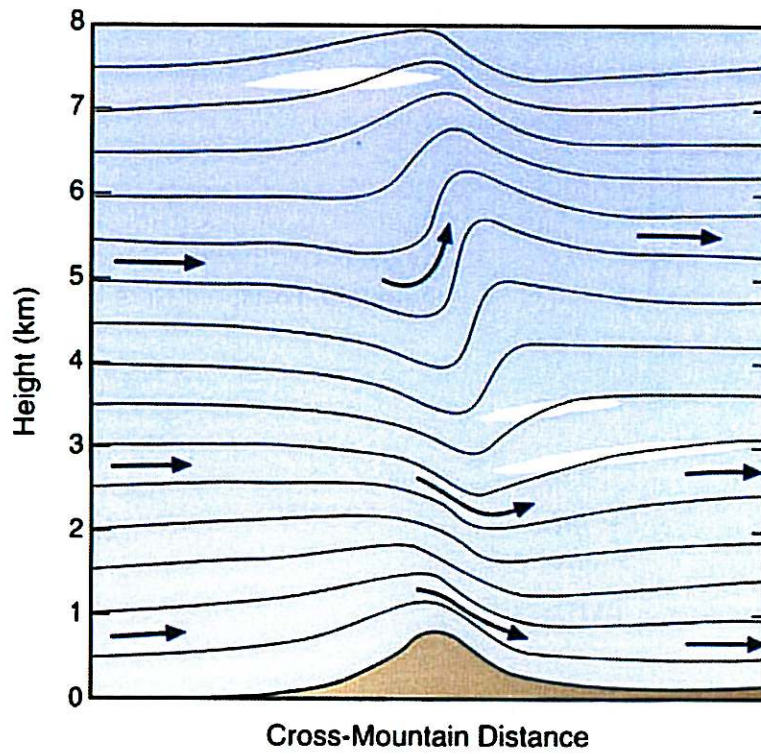


Figure 7: Vertically propagating mountain waves have highest amplitudes far above the mountains. High lenticular clouds are often indicators of these waves. These waves can generate moderate to severe turbulence [Whiteman (2000)].

even in the stratosphere. Waves that form in the lee of mountains are called *lee waves* (see Figure 7). Lee waves are often confined or trapped in the lee of the barrier by a smooth, horizontal flow above. The two types of waves are collectively called *orographic waves* or simply mountain waves. In general, mountain waves are found higher in the atmosphere and tend to have longer wavelengths and smaller amplitudes than lee waves. Orographic waves form most readily in the lee of steep, high barriers that are perpendicular to the approaching flow. The amplitude of the waves, which decays with distance from the mountain barrier, depends on the initial displacement of the flow above its equilibrium position on the windward side of the mountain. In general, the higher the barrier, the greater the amplitude of the waves. If the flow crosses more than one ridge crest, the waves generated by the first ridge can be amplified (a process called resonance) or canceled by the second barrier, depending on its height and distance downwind of the first barrier (see figure 9). The basic form of a wave (trapped or vertically propagating) and its wavelength depend on variations in the speed and stability of the approaching flow. When stable air is carried over a mountain barrier, one of three flow patterns will result, depending on the characteristics of the wind profile.

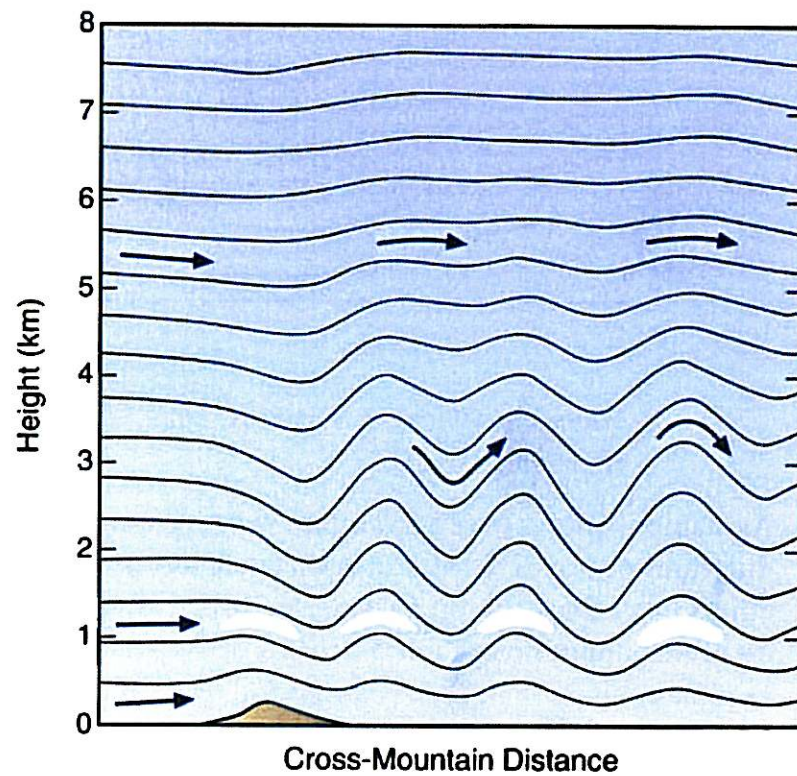


Figure 8: Trapped lee waves reach their highest amplitudes in a confined layer on the lee side of the mountains. Regularly spaced low-altitude lenticular clouds are the best indicators of trapped lee waves. These waves can generate moderate to severe turbulence [Whiteman (2000)].

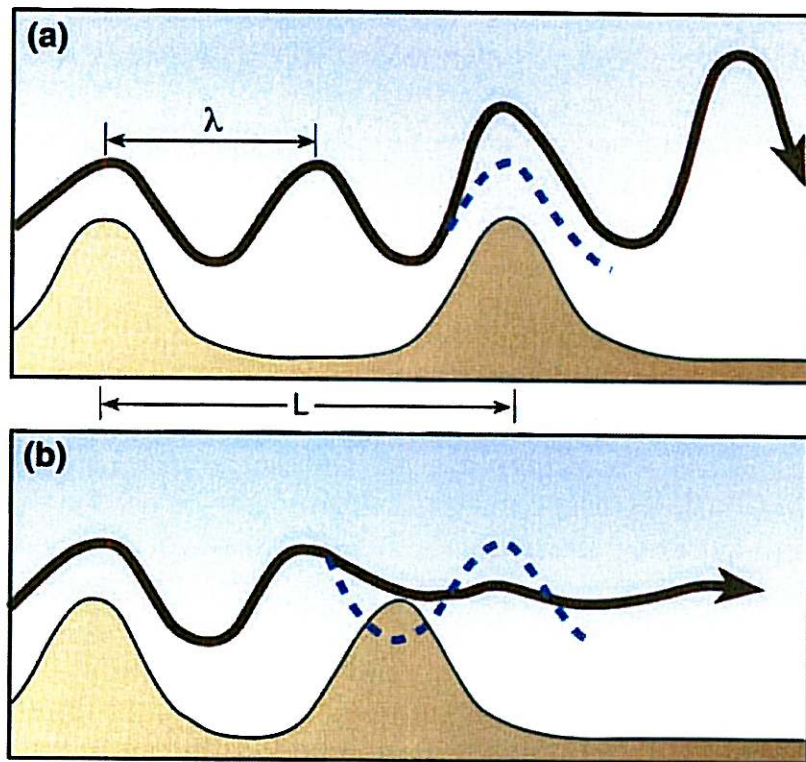


Figure 9: Waves can be (a) amplified or (b) canceled by successive ridges, depending on the relationship between the ridge separation distance L and the wavelength λ of the flow [Whiteman (2000)].

If the winds are weak and nearly constant with height, shallow waves form downwind of the barrier. When winds become stronger and show a moderate increase with height, the air overturns on the lee side of the barrier, forming a standing (i.e., non-propagating) lee eddy with its axis parallel to the ridgeline. When winds become stronger still and show a greater increase with height, deeper waves form and propagate farther downwind of the barrier. Wavelength increases when wind velocities increase or stability decreases.

2.4 Flow around mountains

A flow approaching a mountain barrier tends to go around rather than over the mountains if

- the ridge line is convex on the windward side,
- the mountains are high,
- the barrier is a single isolated peak or a short range,
- the cross-barrier wind component is weak,
- the flow is very stable, or
- the approaching low-level air mass is very shallow.

2.5 Flows through gaps, channels and passes

Strong winds are often present in gaps (major openings through mountain ranges), in channels between mountain subranges, and in mountain passes. The winds are usually produced by pressure-driven channeling, that is, they are caused by strong horizontal pressure gradients across the gap, channel or pass. The pressure gradient may be imposed on the terrain by traveling synoptic-scale pressure systems or may result from differences in temperature and density between the air masses on either side of the opening. The differences are usually caused by regional-scale processes, but may also result from smaller scale processes such as cold thunderstorm outflows. The strongest gap winds occur when synoptic-scale pressure gradients are superimposed on regionally developed pressure gradients. The physical processes are similar for gaps, channels and passes.

2.5.1 Flows through coastal mountain ranges

Regional pressure gradients occur frequently across coastal mountain ranges because of the differing characteristics of marine and continental air masses. In winter, the coldest and densest air is found over the elevated interior of the continent, whereas temperatures on the ocean side are moderated by the open ocean. When the pool of cold air in the interior becomes deep enough, it spills over the lowest altitude gaps, producing strong winds that descend toward the coast. This phenomena is frequently occurring in the mountainous

regions considered in the present analysis during the winter periods. Further deepening of the cold pool increases the flow through the gap and allows air to flow over low ridges and eventually through higher altitude passes. When low clouds are present, the cloud mass fills the gap or pass and descends like a waterfall into the adjacent valley. Because major channels or gaps are generally lower in altitude and wider than passes, they carry the strongest flows and largest air volumes.

In summer, continental interiors are warmer than the adjacent ocean, and pressure gradients develop, forcing air through the gap from the ocean to the interior. Thus, it is typical for regionally driven pressure gradients in gaps to reverse between winter and summer, with the direction of the flow determined by the direction of the pressure gradient, usually toward the ocean during winter and toward the inland areas during summer.

2.5.2 The Venturi (or Bernoulli) effect

When a valley or other channel has a substantial pressure gradient along its length and a topographic constriction at some point along the channel, air is accelerated through the constriction by the pressure drop across the constriction (see figure 10). Acceleration through a terrain constriction is called the *Venturi* or *Bernoulli* effect. The flow speed can be roughly estimated by assuming that the mass of the flow is conserved through the channel, so that speed increases when the cross section of the flow narrows and decreases when the cross section widens. When the pressure gradient across the constriction is weak or the constriction provides a near-total blockage, air may pool behind the constriction rather than accelerating through it.

2.5.3 Forced channeling

Most winds through gaps, channels, and passes are driven by the difference in pressure from one side of the gap to the other. These winds blow across the pressure contours from the area of high pressure to the area of low pressure. Some winds, however, result when strong flows aloft under neutral or unstable conditions are channeled by landform features, such as parallel mountain ranges or valleys. Forced channeling, in contrast to pressure-driven channeling, requires the downward transfer of momentum into the channel from winds aloft that are blowing parallel to pressure contours (see figure 11). Forced channeling often occurs with foehn winds and at high altitudes in the mountains, especially at mountain passes.

2.6 Blocking, cold air damming and obstruction of air masses

A mountain barrier can not only channel an approaching flow over, around, or through gaps and passes in the barrier, it can also block an approaching flow or it can obstruct a shallow, stable air mass that develops on one side of the barrier, channeling it along the foot of the barrier and preventing it from crossing the barrier. Blocking, cold air damming, and obstruction all affect stable air masses and occur most frequently in winter.

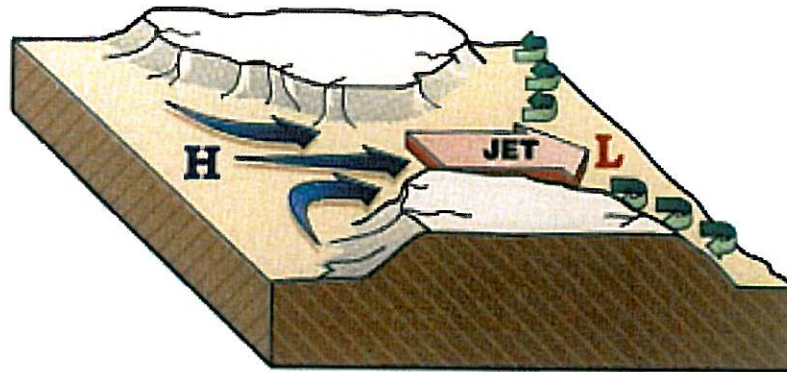


Figure 10: The Venturi effect causes a jet to form as winds pass through a terrain constriction and strengthen [Whiteman (2000)].

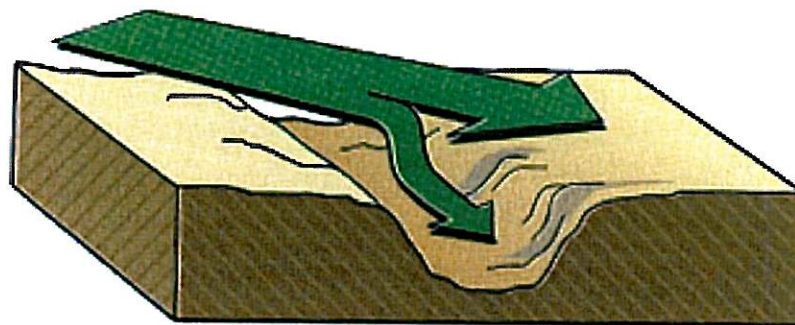


Figure 11: Channeling occurs when upper winds are brought down into valleys from aloft and turned to flow along the valley's longitudinal axis [Whiteman (2000)].

3 Turbulence in the neighborhood of airports

It is reasonable to distinguish between two different phases of landing/take-off when it comes to turbulence.

Turbulence at low altitudes above the airport and its neighborhood This turbulence is mainly determined by or at least influenced by the terrain close to the airport up to a couple of kilometers away, shape of the terrain at the thresholds, the location of hangars and terminal buildings etc. During this phase of the flight the pilot most often can see the airport and its runway. This kind of turbulence is typically a small-scale phenomenon in time and space. The single gust lasts a couple of seconds and is followed by wind speeds below the mean value for some seconds. The more long lasting *wind squalls*, typically lasting for about 1 minute, are most often related to *cumulonimbus clouds*. These clouds are tall and dense clouds often involved in thunderstorms. **This type of turbulence is not predicted by SIMRA.** The reasons for that are the temporal and spatial scales of such phenomena and the lack of modeling variable moisture in the micro-scale region.

Turbulence in the landing/take-off sectors It is impossible to define a strict limit between the previous type of turbulence and the present one, but as a guiding line we talk about turbulence at elevations between 300-400 meters to 3-4 kilometers. The wind measurements on the airport at the runway usually give little or no information about wind fluctuations in the airspace that far away. The turbulence in these areas is mainly determined by the large scale terrain variations in the region. It is often relatively coarse-grained and involves wind fluctuations that are much larger both in time and space. **This type of turbulence is predicted by SIMRA.** Updrafts and downdrafts of air can occur, resulting in significant vertical displacements of an aircraft. The wind and turbulence can be quite complicated. Mountain waves, rotors, vertical and horizontal windshear are often contributing factors.

3.1 Windshear and turbulence

Windshear can be defined as layers or columns of air flowing with different velocities (both speed and direction) to adjacent layers or columns. Windshear is a major hazard for aviation, especially at lower altitudes. Even when flying within a layer with laminar flow and the flight is smooth, the sudden crossing of the boundaries between different laminar airstreams will accelerate/decelerate the aircraft to a greater or lesser degree. Depending on the flight direction relative to the velocity changes, shear may be felt as turbulence, but also as a sudden tail or head wind with respective consequences.

Windshear and convection (vertical thermal convection) are the major sources of turbulence. Basic fluid dynamics tells us that any fluid such as the atmosphere can support only a maximum of shear between laminar flow layers before breaking down into turbulent flow.

Some aircrafts are more effected by turbulence than others. Light aircrafts are effected even by light turbulence, while larger ones are not.

The intensity of turbulence is categorized by ICAO as follows for civil aviation:

Light Effects are less than those of moderate intensity

Moderate • There may be moderate changes in aircraft attitude and/or height, but the aircraft remains in control at all times.

- Airspeed variations are usually small.
- Changes in accelerometer⁴ reading of $0.5 - 1.0 g$ at the aircraft's center of gravity.
- Passengers feel strain against seat belt. There is difficulty in walking. Loose objects move around.

Severe • Abrupt changes in aircraft attitude and/or height. The aircraft may be out of control for short periods.

- All speed variations are usually large.
- Changes in accelerometer readings greater than $1.0 g$ at the aircraft's center of gravity.
- Objects are forced violently against seat belts. Loose objects are tossed about.

Extreme Effects are more pronounced than for severe turbulence.

During previous work we have estimated $3.0 < \sqrt{K} < 4.0$ to be within the range of severe turbulence.⁵

3.2 Horizontal and vertical windshear and effects on aircrafts

Windshear is a difference in windspeed and wind direction over a relatively short distance in the atmosphere. Windshear can be broken down into vertical and horizontal components, with horizontal windshear seen across fronts and near the coast and vertical windshear typically near the surface.

Windshear is a micro-scale meteorological phenomenon occurring over a very small distance. However, it can also be associated with mesoscale or synoptic scale weather features such as squall lines and cold fronts. It is commonly observed near microbursts and downbursts caused by thunderstorms, fronts, areas of locally higher low level winds referred to as low level jets, near mountains, radiation inversions that occur due to clear skies and calm winds, buildings and wind turbines. Windshear has a significant effect during take-off and landing of aircraft due to their effects on control of the aircraft, and has been a significant cause of aircraft accidents in the past (see Figure 12).

⁴An accelerometer measures *weight per unit (test)mass*, also called the *g-force*

⁵ K =Turbulent kinetic energy, \sqrt{K} [m/s] often called *turbulent velocity*

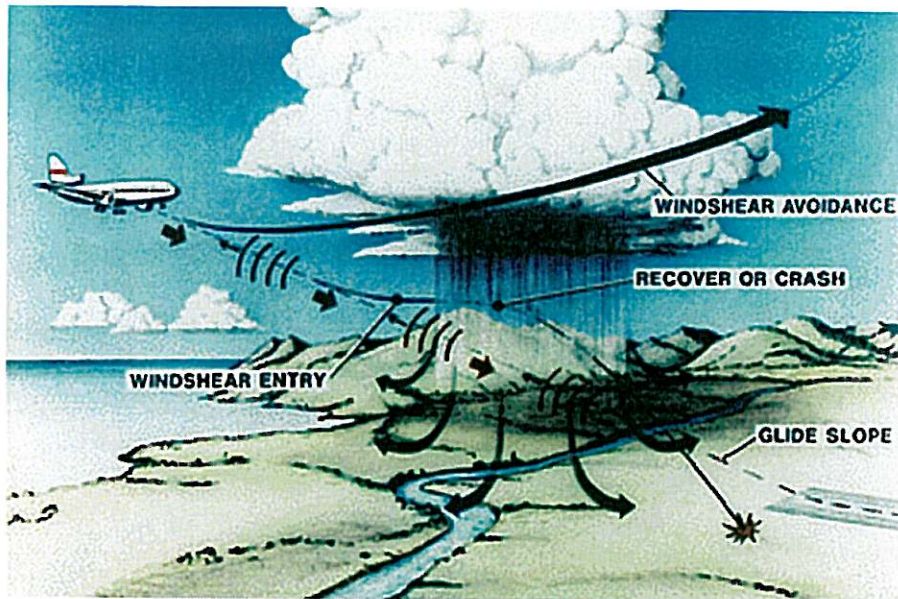


Figure 12: Sketch showing affect of windshear during aircraft descent into an airport (NASA) (Ref. <http://en.wikipedia.org/wiki/File:Windshearaircraftnasa.gif>)

Wind variability is an everlasting and inescapable problem for aviation. Meteorological circulations and terrain-induced airflows can occasionally induce large and rapidly changing variations in the air velocity over small distances. These variations produce correspondingly sudden changes in the relative flow of air over the wings and other lifting parts of an aircraft, resulting in changes in it's flight path. See Figures 13 and 14 for illustration of aircraft's reaction to horizontal and vertical windshear, respectively.

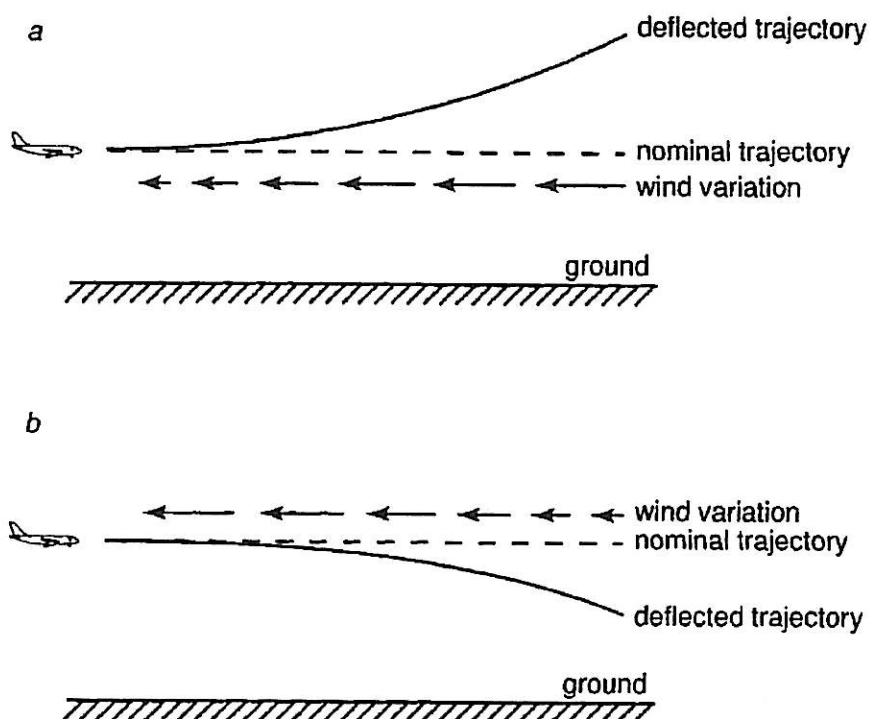


Figure 13: Horizontal windshear and its effect on an aircraft's flight path.

4 Optimizing local forecast regions

In the forthcoming sections of the report we describe the results of optimizing domains and grids for selected Norwegian airports. The approach is characterized by the analysis of the effects of topography and critical wind directions by conducting carefully planned simulations with different boundary locations, boundary orientations and grid resolutions. Finally, the results are compared, focusing on aircraft gliding paths and runway thresholds of the different airports.

However, first a section on digital elevation data is included. So far all existing airport micro-scale forecast regions, mentioned in the Section 1, have been based on regional height-maps with a horizontal resolution of $100 \times 100 m^2$. In order to investigate if this resolution is sufficient, terrain height-maps with a horizontal resolution of $10 \times 10 m^2$ were utilized for all the four airport regions considered. Generally, all four *zones* of a *Digital Elevation Model* (DEM) may be needed to cover an actual micro-scale forecast region. The zones of the Værnes region are illustrated in Figure 15. In this case only the two lower sub-domains are needed. However, all four sub-domains may be needed if the actual airport lays close enough to the cross-point of the four sub-domains. It should also be mentioned that the sub-domains have a 41 grid-lines *overlap* in each direction. This has to be taken into account

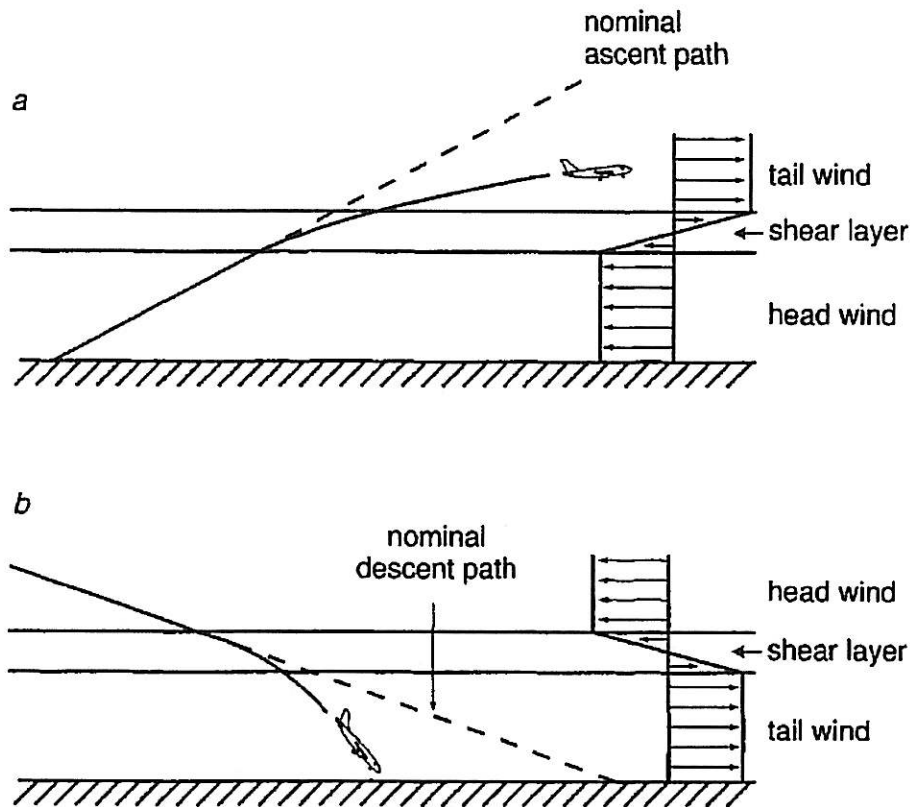


Figure 14: Vertical windshear and its effect on an aircraft's flight path.

when extracting an actual forecast region.

After making the necessary preprocessing of the terrain data, the actual forecast region is chosen with a given resolution. Since it is convenient to be able to choose a slightly coarser resolution than the inherent one, the preprocessing software that is developed facilitates the options $10 \times 10 m^2$, $20 \times 20 m^2$, $40 \times 40 m^2$, $80 \times 80 m^2$ and $160 \times 160 m^2$ of terrain resolution.

4.1 Digital elevation models

A digital elevation model (DEM) is a digital model or 3D representation of a terrain's surface, created from terrain elevation data.

A DEM can be represented as a raster which a grid of squares, also known as a height-map when representing elevation, or as a triangular irregular network (TIN). The TIN DEM dataset is also referred as a primary (measured) DEM, whereas the Raster DEM is referred as a secondary (computed) DEM. DEMs are commonly built using remote sensing techniques, but they may also be built from land surveying. DEMs are used often in

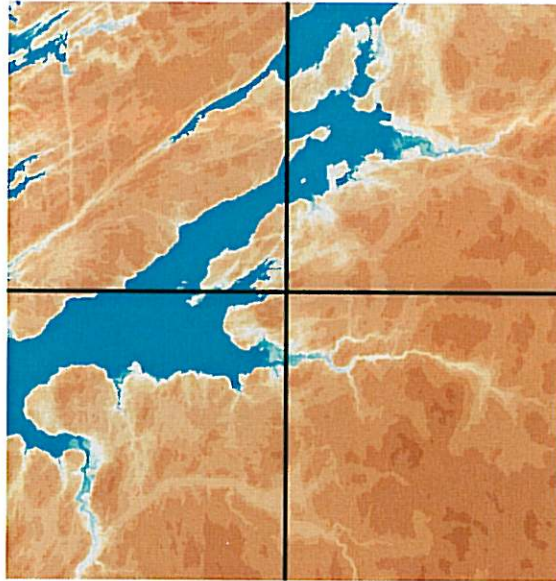


Figure 15: Digital terrain data for the *Værnes* region. The plot is using a logarithmic scale in order to highlight lower elevations.

geographic information systems, and are the most common basis for digitally-produced maps.

As mentioned above, in this study DEM data that are fine-scaled ($10 \times 10 m^2$) have been utilized. Avinor has supported the project team with detailed terrain data for all four airport regions (Hammerfest, Trømsø, Sandnessjøen and Trondheim) under investigation. Since all the necessary preprocessing software is developed, other airport regions are readily analyzed in the same manner.

4.2 Airflow simulation code

The in-house CFD code *SIMRA*⁶ was used to generate all the results that are presented in this report. The version used is a different version from that used in terrain-induced turbulence forecasting. However, the differences are minor and mainly the feature that the forecast version is a single-block structured grid code, while the version used for the present investigations is a fully unstructured grid code. Readers that are interested in details regarding these matters as well as details regarding mathematical modeling of turbulent geophysical flow and numerical approximation and solution of the resulting equations implemented in *SIMRA* are referred to [Utne (2007a)], [Utne (2007b)] and [Utne (2006)].

⁶Semi Implicit Method for Reynolds Averaged Navier-Stokes equations

4.3 Results of studying four Norwegian airports

Here is described the findings of analyzing the existing forecast regions and grids for different city airports (Trondheim, Sandnessjøen, Tromsø and Hammerfest), studying the topography around each one. Thereafter, critical wind directions are depicted and selected simulations are performed for different boundary locations, orientations, and grid resolutions. Finally the results are compared, focusing on aircraft glide paths, thresholds and landing spots on the runway. Information about wind conditions at many Norwegian airports was collected and reported in the late seventies and some of this information is include in this report (see [Dannevig & Hoem (1979)]).

4.3.1 Trondheim Airport Værnes - 17 m ASL RWY 09/27

The topographic conditions are complicated and rather different north and south of *Trondheimsfjorden*. The mountains to the south of the fjord are barriers for strong southerly winds which are likely to channel airstreams down through valleys and other areas that are less obstructive to the airflow. Prevailing wind directions during winter are out of fjords and down valleys, the direction often being SW to SE. Very often this is cold air drainage from inland areas. During summer the surface winds are most often inwards the fjords which results in westerly wind for Værnes. Westerly winds are also the dominating height wind direction all through the year.

Værnes may have difficult landing conditions at strong southerly winds. The runway is located close to the fjord, part of it actually in the fjord. The nearby area is relatively flat while there are tree growing hills father away from the airport. As close as 2 km to the southwest the hills are about 250 m high. The valley *Leksdalen* to the south, oriented NNW-SSE, has a significant airflow channeling effect. Moderate turbulence often occurs for southeasterly to southwesterly winds exceeding 10 m/s. Strong turbulence can occur for wind speeds over 20 m/s, in particular when combined with low *atmospherical stability*. The surface winds in these situations are S-SE and very *gusty*. In cold weather with *inversions*⁷ the surface winds may be weak, but at the same time there are regions with windshear and turbulence a few hundred meters above the ground. In situations with turbulence the maximum gust may be stronger than indicated by the wind field. The conditions are worse on the south side than on the north side of the location and the conditions are often made even worse by side winds at the runway.

In the *Gråkallen* area where the approach of landing is often performed, at strong wind fields severe turbulence can be experienced at elevations as high as 4000 m. In some situations with southwesterly wind fields, strong windshear and turbulence may even occur below elevations of 1000 m. *Downdrafts* may occur at the threshold on the east side of the runway when the wind is westerly and quite strong. For further information on the special conditions at this airport it is referred to [Dannevig & Hoem (1979)].

⁷A deviation from the normal change of an atmospheric property with altitude. Most often it refers to a temperature inversion, i.e. an increase of temperature with height

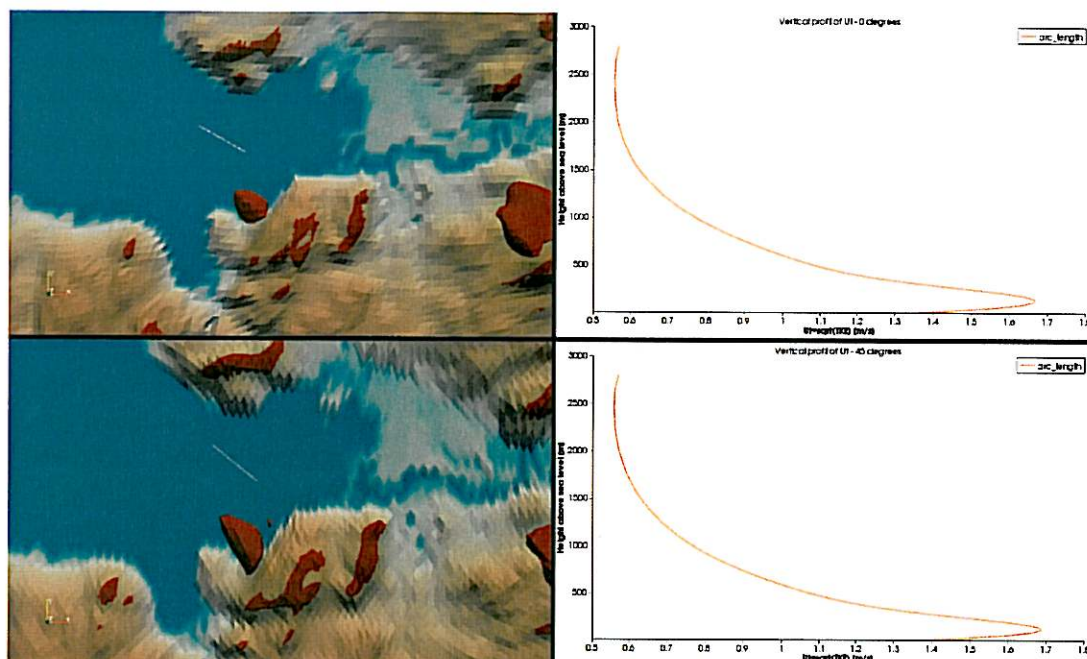


Figure 16: This figure shows the results of analyzing the sensitivity to regional rotation at Værnes. The upper left and lower left images show iso-surfaces of turbulent velocity indicating moderate turbulence to severe turbulence for no rotation and a counterclockwise rotation of 45° , respectively. The curves on the right side show the associated turbulent velocities for both cases along a vertical line located in the fjord right through the gliding path of aircrafts approaching the runway from the west. Note the larger extent of the turbulence area as well as the larger maximum value of the turbulent velocity in the case of regional rotation.

4.3.2 Sandnessjøen Airport Stokka - 17 m ASL RWY 03/21

The airport lays on a relatively plane area close to the sea with a runway oriented parallel to the coast line. To the east there is a hilly terrain with heights up to 150 meters. At a distance of about 5 kilometers to the east-southeast *De syv søstre* are found which is a craggy mountain ridge that rises approximately 1000 meters. This ridge and its peaks are significant turbulence generators that may cause problems when the wind blows from southeast. In that case, moderate turbulence is common, and the turbulence may be severe at elevations between 1000 and 2000 meters for stronger wind speeds. The turbulence is damped significantly below 200 meters ASL. The surface wind is very uneven under such conditions. The mean wind speed is often low, but at the same time there are gusts with variable wind directions between east and south. Due to the turbulence generators (*De syv søstre*), SE is a very unstable wind direction at the Stokka airport. Moderate turbulence occurs at strong westerly wind fields when airplanes are landing at RWY 21.

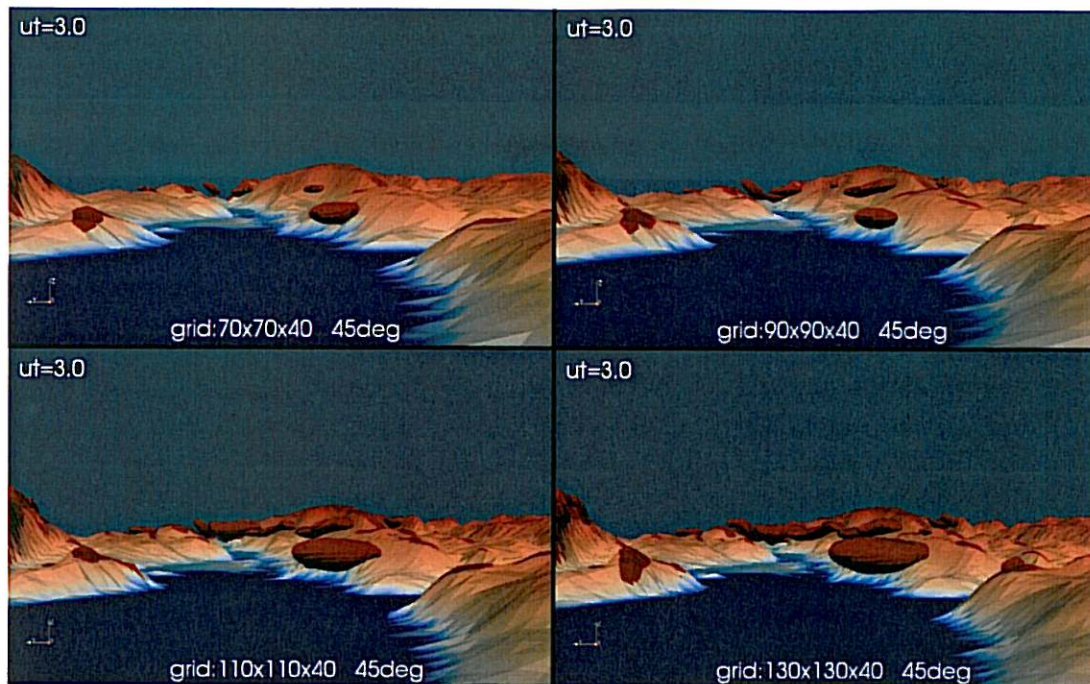


Figure 17: The figure shows topography around the airport at Værnes looking towards the valley *Stjørdalen*, and turbulent velocity iso-surfaces ($ut=3.0$) using four different grid resolutions. Typically, doubling the grid density horizontally makes a significant improvement to north of the hillside *Gjevingåsen* and further east into the valley of *Stjørdalen*. These areas are crossing the approach path of aircrafts both on the western and the eastern side of the airport.

4.3.3 Tromsø Airport Langnes - 10 m ASL RWY 01/19

The airport lays on a relatively flat area on the western side of island *Tromsøya* and have thresholds going almost out in the sea on both ends of the runway.

At larger distances there are mountains with peaks rising more than 1000 meters. These mountains are oriented in the direction SSW-NNE. Also the coastline is oriented this way even though it is quite uneven.

In this area moderate turbulence is quite common all the way up to 2000 meters of elevation when the wind is strong, in particular in the SW-NW sector. In addition, these airstreams are often unstable and can give squally side-winds at the runway. The turbulence can in some cases give problems at approach and landing. Due to channeling effects the wind may be SSW with moderate strength at the runway, while there is a significant windshear 100 m meters above the ground. Pilots have registered significant losses of height due to sudden tailwind at elevations of 6-700 meters and strong wind-fields (WSW and about 50 knots). In [Dannevig & Hoem (1979)] this phenomena is assumed to be connected to a large-scale and complicated terrain-forced wind-field. During the present work this explanation was hard

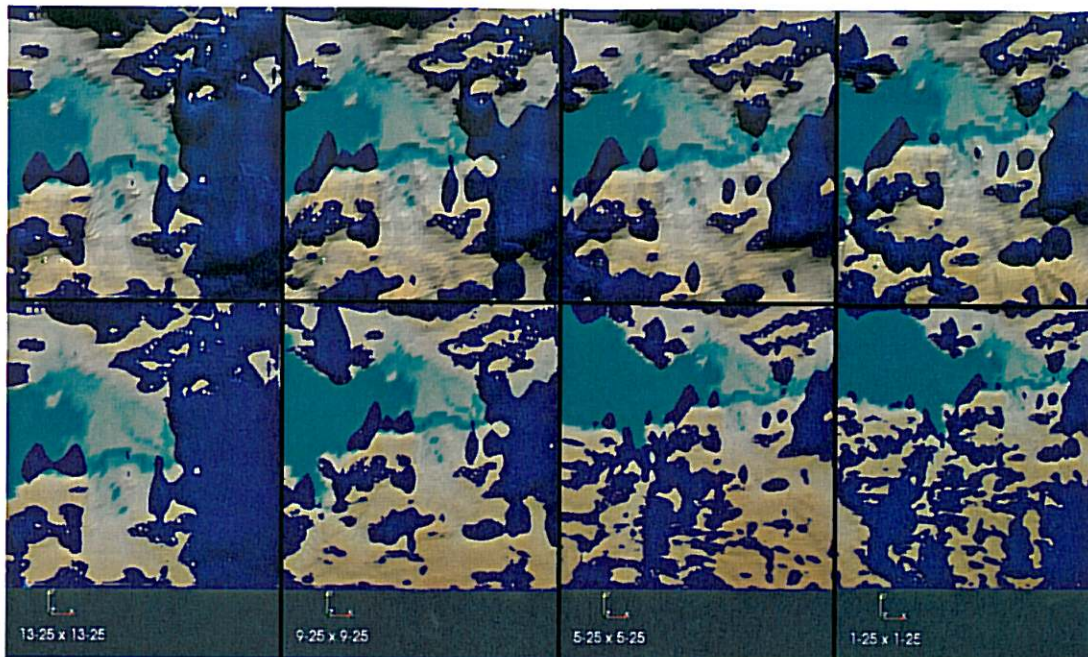


Figure 18: This figures illustrates the sensitivity of predicted turbulent velocity to the size and location of the forecast region at Værnes. From left to right the regions are 12×12 , 16×16 , 20×20 and 24×24 kilometers of extension horizontally, all of which coincide in the north-east corner.

to confirm even though it was initially considered to be a significant factor. An additional factor was also mentioned in [Dannevig & Hoem (1979)], that of passages of squall clouds, resulting in a sudden change of surface wind direction to W-NW. This kind of phenomena is outside our scope of investigation.

4.3.4 Hammerfest Airport - 81 m ASL RWY 05/23

The airport is sheltered by mountains more than 300 meters high and quite close on the NW side. There are some more distance to the mountains in the NE-SE sector. In the SW direction the terrain is open with a relatively steep slope down to the sea right outside the threshold to lane 05.

Of importance for turbulence conditions at this airport is the fact that the mountains on the NW side implies a significant channeling effect in the direction SW-NE, which also coincides with the direction of the coastline. Remember that the coastline very often directs the larger-scale airstreams along the coast. The fjord (*Straumen*) with its neighboring terrain give a guiding or channeling of the airstreams in S-N direction. This is particularly true with wintery conditions and drainage of cold air from the inland areas.

Moderate to strong turbulence at relatively low altitudes is common with height winds

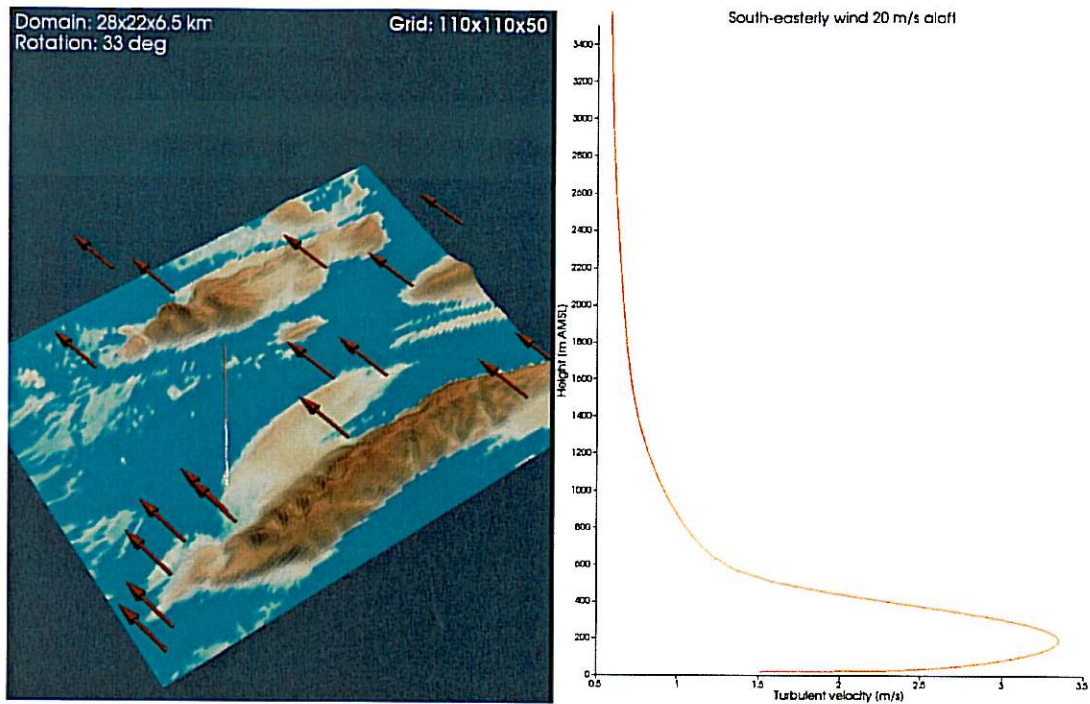


Figure 19: The figure illustrates a worst case scenario at Stokka when strong wind is forced to cross over the relatively long, high and "wavy" mountain-ridge of *De syv søstre*. The simulation is done without atmospheric stratification. With a stable atmosphere, mountain waves are easily generated with *rotors* on the lee side of the mountain, resulting in severe turbulence.

between W and N. The vertical component of the airstream is hardly damped at all during approach and landing at 05. Downdrafts and significant windshear can also occur. In particular, with strong wind speed and wind directions in the sector $270^{\circ} - 300^{\circ}$, the flight conditions may be quite difficult.

For strong SE wind-fields moderate turbulence may occur over a large area. This is probably due to a channeling effect combined with the blocking effect of the mountains on the NW side of the airport.

Hammerfest is probably the most difficult airport in *Finnmark* when it comes to terrain-induced turbulence.

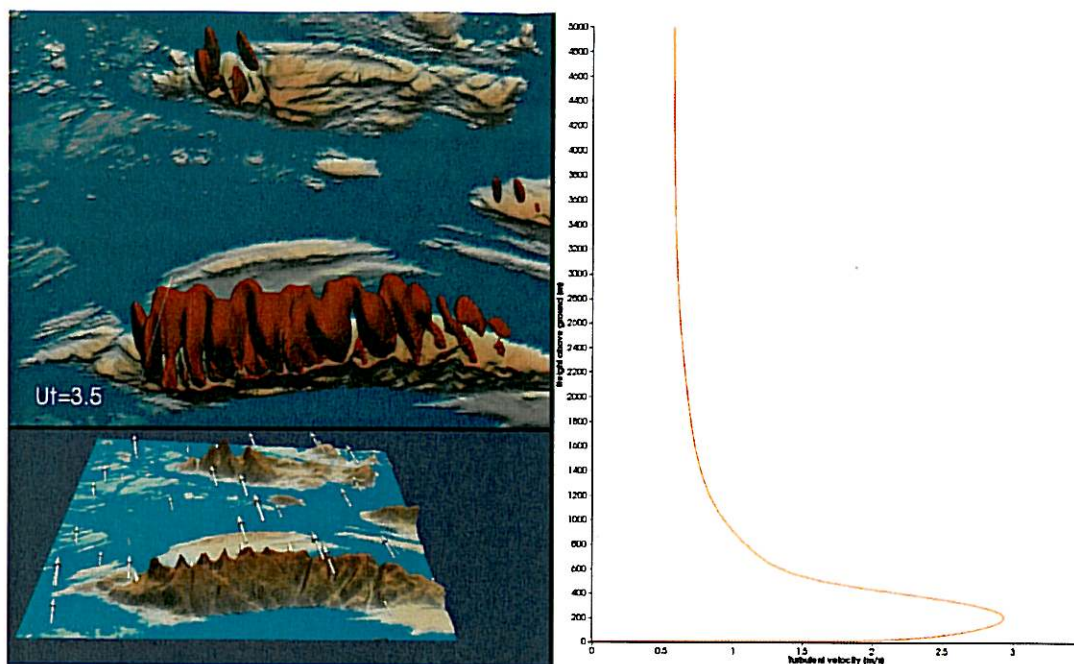


Figure 20: This figure shows terrain and predicted severe turbulence ($ut=3.5$) at Stokka for south-easterly wind crossing the mountain-ridge with speed 20 m/s aloft. Neutral atmosphere.

5 Conclusion

The general conclusion after studies of topography around a number of Norwegian airports that presently get regular operational forecasts of terrain-induced turbulence, is that there is a potential for improving both computational efficiency, robustness and accuracy of the forecast by optimizing regional shape and size of the local forecast area as well as the quality of the micro-scale grid within that area. However, there are important requirements and limitations posed by the operational forecast computer system: the computations need to be completed in a given time frame. Since 2005 when five airports in Norway had their first turbulence forecast system installed in test mode, the power of the *number-crunching* computers used for this purpose has continuously increased. Next year there will a significant upgrade of the *supercomputer* running the whole nested forecast system, which opens for utilizing finer and larger grids for airports with topography that are not resolved with the present models and grids.

It must be mentioned that there are airports that have different characteristics that are related to the meteorology not resolved in the SIMRA model. Examples are *squalls* and (vertical) thermal convection and turbulence. We should also mention smaller spatial and

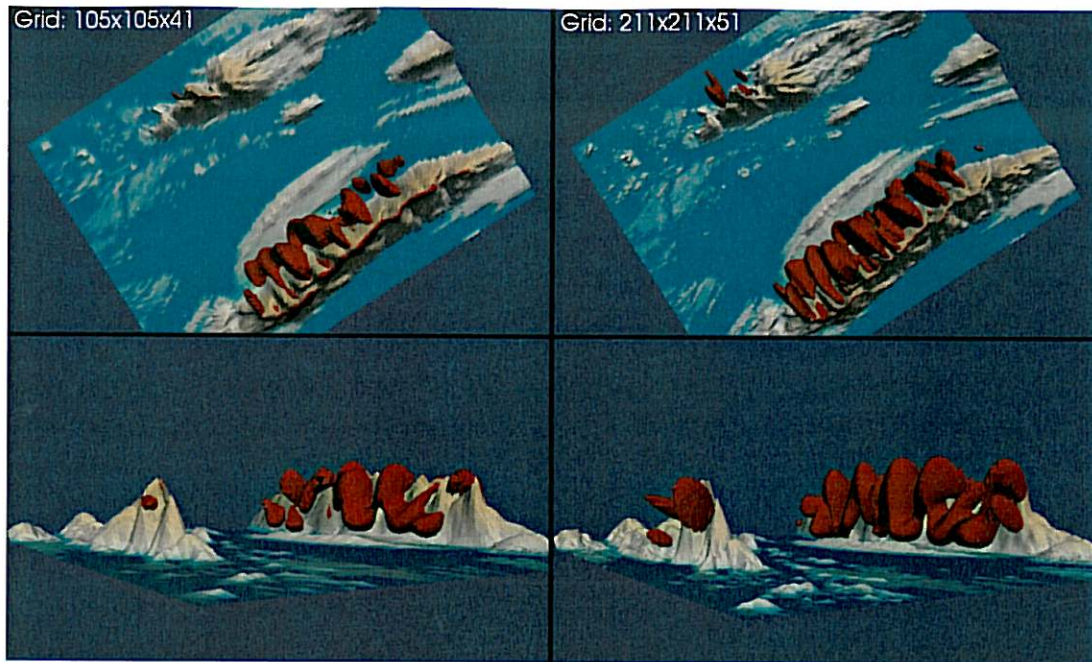


Figure 21: Sensitivity of turbulence velocity to grid density at Stokka. A doubling of the number of grid points horizontally (both directions) and increasing the number of grid points vertically by a factor 1.25, "moves" the severe turbulence zones closer to the airport. Also note the wavy turbulent regions over the mountain-ridge.

time scale phenomena not resolved by the RANS⁸ type model of the SIMRA code, like buildings close to the airport/runway and gusts generated on a time scale of a few seconds. However, the development of more powerful computers and the continuous development of more advanced turbulence models give promise to capture even finer details in a turbulence forecast system like the present one in the future.

When it comes to the findings for the airports studied during the present work, a general comment concerns the grid density of the SIMRA regions enclosing the airports investigated. A doubling of the number of grid points horizontally and increasing the number of grid points vertically by a factor of 1.5, are recommended. The extra grid points both vertically and horizontally should mainly be put close to mountains in order to improve the capturing of mountain waves and rotors. The latter phenomena are quite important during periods of atmospheric stratification and are significant turbulence generators. This level of grid improvement is believed to be realistic during next year with the upgrade of the computer running the whole nested forecast system for weather and turbulence.

The present SIMRA forecast region for *Trondheim Airport Værnes* should be extended to the east in order to give turbulence forecasts related to the mountain ridge on the south

⁸ RANS=Reynolds-Averaged Navier-Stokes

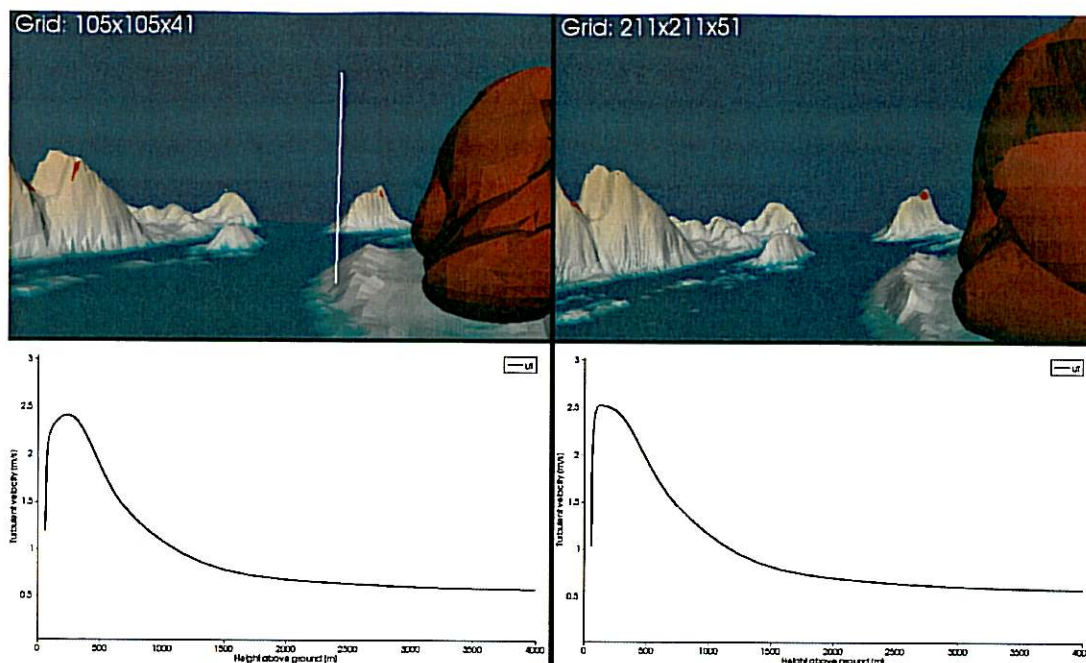


Figure 22: This shows a close-up of the results of Figure 21 for Stokka airport. Note the approaching front of severe turbulence resolved by the finer grid of $211 \times 211 \times 51$ points. Also note the sharper and higher peak of the turbulent velocity curve along a vertical line approximately at the middle of the runway location, for the denser grid case.

side of the valley *Stjørdalen* and wind in the sector S-SE. The area north of the hillside *Gjevingåsen* in the approach and landing path of aircrafts should be better resolved. Experiments have shown that the regions of severe turbulence generated by this hillside for strong winds in the sector SW-SE, are cut-off too early due to coarse grid resolutions of the present system. The small rotation of the forecast region was tested and compared with the present non-rotated one. The rotation was done in order to line-up grids with the mountain ridges that occupy the area, though not being very dominant. The results showed a slight improvement for the southeasterly wind direction. Some of the changes for Værnes will be implemented in near future.

The present forecast region for *Sandnessjøen Airport Stokka* is rotated approximately 33° . This was done initially to line-up with the mountain ridge called *De syv søstre*. Some tests were done in order to decide on the optimal value of rotation. In this case, the *method of sensitivity* mentioned in Section 1, would have been an appropriate tool. Our present tests could not depict any rotation angle that was better than the existing one (33°) for critical wind directions. The main issue with *Stokka* is the grid resolution on the western side of this relative high (more than 1000 m ASL) and "wavy" mountain ridge. Our experiments show that grid resolution on the lee side (assuming land winds) of these mountains is quite critical when it comes to the predicted extent of severe turbulence regions in these areas. It

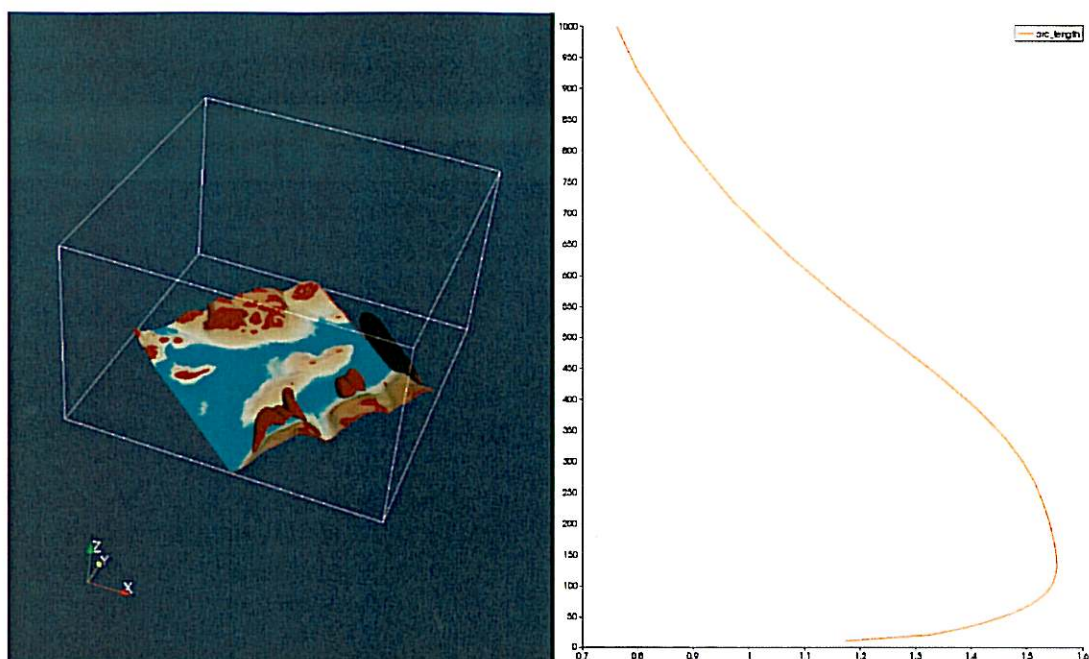


Figure 23: Initial simulation of terrain-induced turbulence at Langnes in Tromsø. Note that close to light turbulence is predicted at higher elevations than for the previous airports. The curve on the right side shows turbulent velocity along a vertical line located at the runway.

is recommended to make an extended effort to make a local refinement of the grid all along the ridge between the ridge and the sea on the western side. If a new runway is established closer to the sea, this recommendation is still valid.

The turbulence forecast region for *Tromsø Airport Langnes* has many channeling features (several islands and fjords) that complicate the forecasts. Sudden change of wind direction in the sector SW-NW seems to be a special problem since windshear and turbulence can occur due to channeling of airstreams through fjords and between mountains. In this case the micro-scale code SIMRA is very much dependent on the meso-scale code (presently UM1). The mountains are oriented in the direction SSW-NNE which indicate that a certain rotation of the forecast region should be done. Our preliminary tests show no significant improvements by such a procedure, but this needs to be investigated further.

Hammerfest Airport was the actual airport triggering the onset of the present turbulence forecast system, due to an event back in 2005. This airport is regarded to be the most difficult airport in the region. As for all of the other airports investigated the grid resolution is important. In particular this is true along the valley in the direction of the runway and on the slopes of hillside on the NW side of the airport. Considerations regarding local grid refinement on the SE side of the airport should also be done. The preliminary tests show promise of improvement in doing so. Rotation of the SIMRA forecast region to line-up with the hillside on the NW side of the airport shows some improvements.

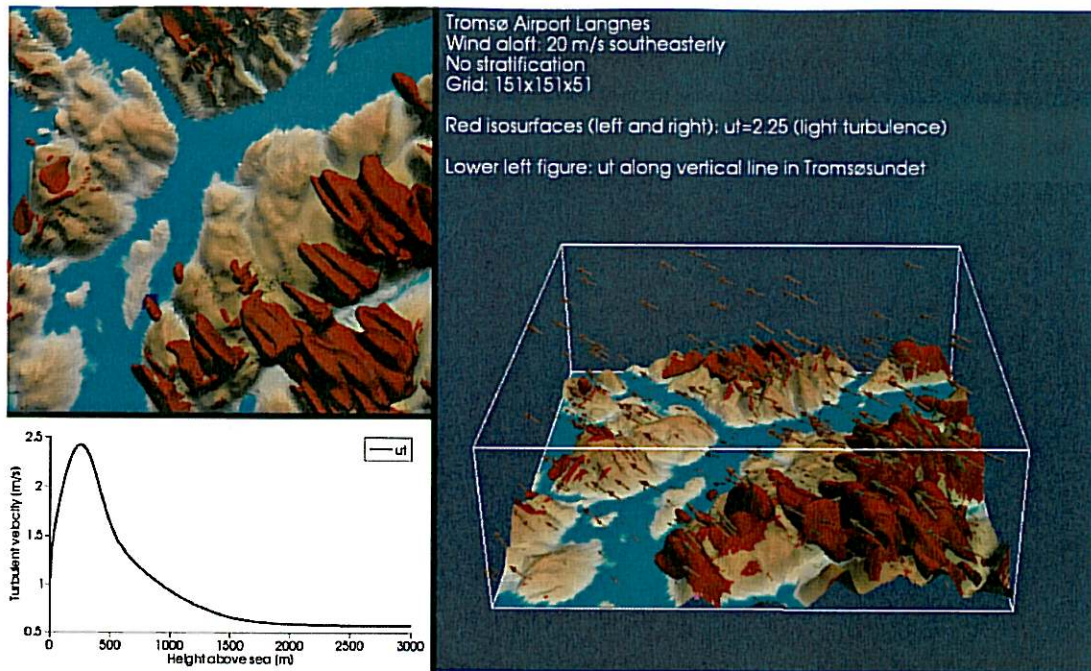


Figure 24: This figure shows terrain and regions of light to moderate turbulence at Langnes. Further explanations in the figure.

Acknowledgement

We are thankful to Mariann Nilssen at Avinor for providing detailed terrain data for the selected airport regions which formed the basis of the present study. We are also thankful to Erling Bergersen for giving his feedback on airport selections and the form of the resulting report. Thanks are also due to Helge Midtbø for interesting and valuable discussions regarding meteorological processes that are important in the present context. We would also like to thank Marit Ødegard for giving this report the final touch.

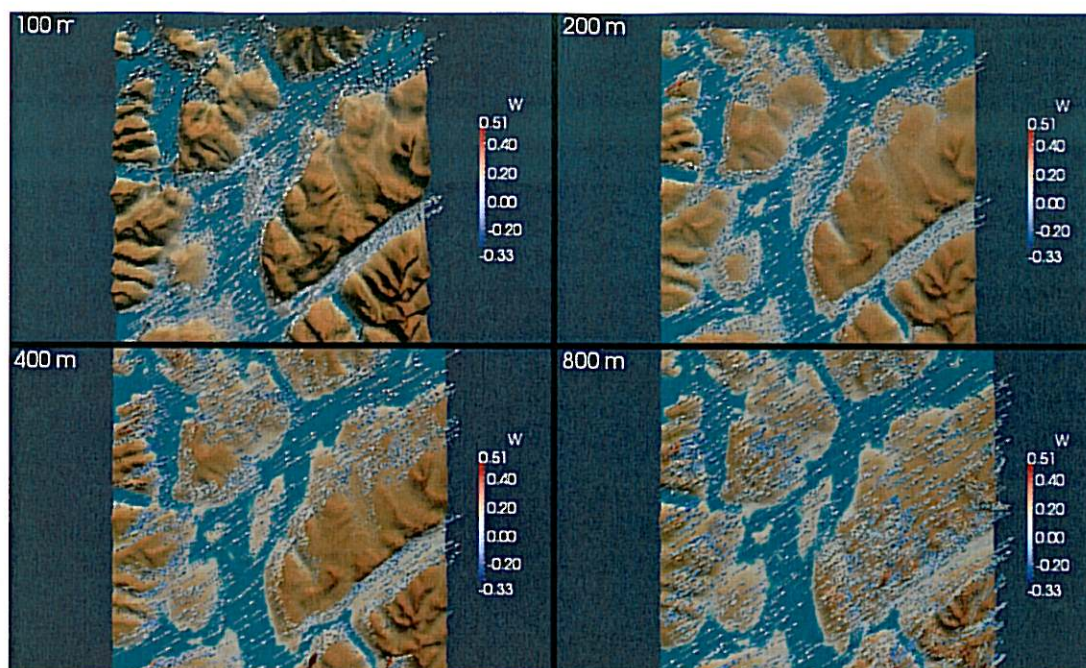


Figure 25: Trossø Airport Langnes. West-southwesterly wind 20 m/s aloft and idealized wind profile at inflow boundaries. Illustration of the channeling effect at different levels. Also note the variation of the vertical component at the various levels.

References

- [Dannevig & Hoem (1979)] P. Dannevig, V. Hoem: Turbulensforholdene ved norske flyplasser, (in Norwegian), Technical Report no 30, Det Norske Meteorologisk Institutt
- [Eidsvik & Holstad & Lie & Utne (2004)] K.J. Eidsvik, A. Holstad, I. Lie, and T. Utne 2004: A prediction system for local wind variations in mountainous terrain. *Boundary-Layer Meteorology*, Vol. 112, No. 3, pp. 557-586.
- [Eidsvik & Utne (2006)] K.J. Eidsvik, T. Utne 2006: Vindvariasjoner over Hammerfest lufthavn basert på estimater for 01-05-2005 kl 1400, (in Norwegian), *SINTEF Report A161*.
- [Eidsvik (2006a)] K.J. Eidsvik 2006: Prediction errors associated with sparse grid estimates of local atmospheric flows, *SINTEF Report A184*.
- [Eidsvik (2006b)] K.J. Eidsvik 2006: Predictions of local atmospheric flows based upon Reynolds-averaged equations, applied to aviation safety, *SINTEF Report A185*.
- [Eidsvik (2006c)] K.J. Eidsvik 2006: Prediction of local flow in mountainous terrain, *SINTEF Report S903*.

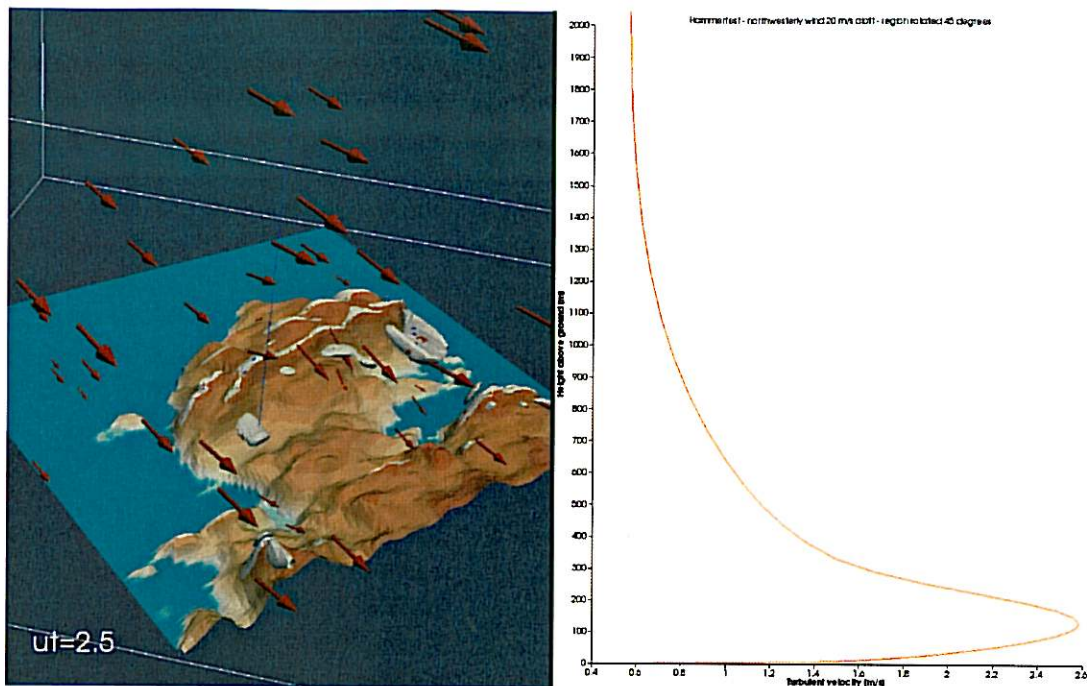


Figure 26: Terrain and predicted turbulent regions at Hammerfest Airport for north-westerly winds crossing the hillside on the NW side of the airport. A region of moderate turbulence is predicted at the location of the runway.

- [Eidsvik (2008)] K.J. Eidsvik 2008: Prediction errors associated with sparse grid estimates of flows over hills, *Boundary-layer Meteorology*, Vol. 127, No. 1, pp. 153-172.
- [Utne (2006)] T. Utne 2006: Segregert implisitt algoritme for løsning av Navier-Stokes og Reynolds ligninger, (in Norwegian), *SINTEF Report A171*.
- [Utne (2007a)] T. Utne 2007: Modelling of Stratified Geophysical Flows over Variable Topography, *Geometric Modeling, Numerical Simulation, and Optimization: Industrial Mathematics at SINTEF*. Springer, Berlin.
- [Utne (2007b)] T. Utne 2007: A Segregated Implicit Pressure Projection Method for Turbulent Flows, *SINTEF Report A1686*.
- [Utne & Sørli (2008)] T. Utne, K. Sørli 2008: Metoder for lokal data-assimilering relatert til varsling av turbulens ved flyplasser, (in Norwegian), *SINTEF Report A7333*.
- [Utne & Sørli (2009)] T. Utne, K. Sørli 2009: Lokal data-assimilering i SIMRA: Korreksjon av vindstyrke og retning ved bruk av flydata, (in Norwegian), *SINTEF Report A11931*.

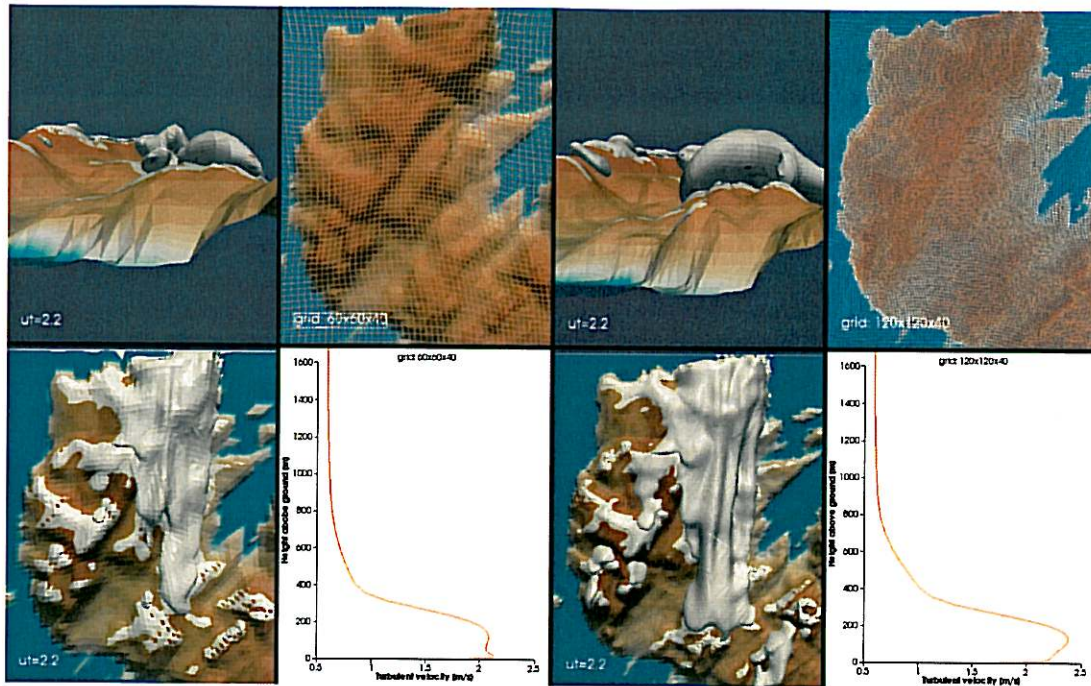


Figure 27: Sensitivity of turbulent zones to grid density at Hammerfest Airport. Note the different maximum values of turbulent velocity along a vertical line at the airport for the coarse and fine grid.

[Whiteman (2000)] C. D. Whiteman: Mountain Meteorology, Fundamentals and Applications, Oxford University Press, 2000

